Solar Energy 220 (2021) 635–649

Contents lists available at ScienceDirect

Solar Energy

journal homepage: www.elsevier.com/locate/solener

Fabrication analysis of flat vacuum enclosures for solar collectors sealed with Cerasolzer 217

Farid Arya [a,*], Trevor Hyde [b], Paul Henshall [c], Philip Eames [d], Roger Moss [e], Stan Shire [e], James Uhomoibhi [f]

[a] School of Engineering, Buckinghamshire New University, UK
[b] Centre for Sustainable Technologies, Ulster University, UK
[c] School of Architecture, Oxford Brookes University, UK
[d] Centre for Renewable Energy Systems Technology, Loughborough University, UK
[e] School of Engineering, University of Warwick, UK
[f] School of Engineering, Ulster University, UK

ARTICLE INFO

Keywords:
Vacuum enclosure
Solar absorber
Vacuum insulation
Evacuated flat plate solar collector
Ultrasonic soldering

ABSTRACT

Vacuum flat plate (VFP) solar thermal collectors exhibit excellent optical and thermal characteristics due to a combination of wide surface area and high vacuum thermal insulation offering a high performance and architecturally versatile collector with a variety of applications for industrial process heat and building integration. A vacuum flat plate solar collector consists of a solar absorber in a flat vacuum enclosure comprising glass or glass and metal covers sealed around the periphery with an array of support pillars to maintain the separation of the enclosure under atmospheric pressure. The edge seal must be both mechanically strong and hermetic to ensure the durability of the internal vacuum over collector lifetime. This presents several challenges for the fabrication of flat vacuum enclosures. In this study a novel sealing technique is presented using a tin-based alloy, Cerasolzer 217, to create the vacuum seal between two glass panes and an edge separating spacer. The sealing process is undertaken at temperatures $\leq$250 °C allowing the use of thermally tempered glass panes. The mechanical strength of the edge seal was investigated using a tensometer. It was demonstrated that the bond between glass and edge spacer was sufficiently strong to withstand induced stresses in the edge seal region. The edge seal was leak tested using a conventional Helium mass spectrometer leak detector and was shown to possess leak rates low enough to maintain an adequate vacuum pressure to supress conductive and convective heat transfer in the collector. A finite element method (FEM) is developed and validated against the experimental results and employed to predict the stresses in different regions of the enclosure. It was found that the mechanical strength limits of the seal and glass are higher than the stresses in the edge seal region and on the glass surface, respectively.

1. Introduction

Flat vacuum collectors are highly efficient and provide an architecturally attractive solution for researchers and industry in construction and energy sectors worldwide (Arya et al., 2018a; 2018ba, 2018bb, 2018cc, 2018dd, 2018ee, 2017f; Moss et al., 2018a). These collectors have a larger surface area available for heat collection in comparison with conventional vacuum tube collectors (Beikircher et al., 2015). In addition, they are potentially slimmer and architecturally appealing making them suitable for applications in the cladding of building façades. As well as generating thermal energy, vacuum flat plate collectors can provide solar shading in summer and contribute to building thermal insulation, lowering carbon emissions.

A flat plate collector for high efficiency at medium temperatures (70–120 °C) was proposed (Beikircher et al., 2015) where multiple transparent glass panes were used to divide the space between the cover glass and the solar absorber to minimise convective heat loses. The thermal insulation properties of air, Krypton and arogel at low pressure ranging from 1 KPa to 10 KPa in a vacuum flat plate collector was investigated (Benz et al., 1996). One of the main issues identified in this

* Corresponding author.
E-mail addresses: farid.arya@bucks.ac.uk (F. Arya), t.hyde@ulster.ac.uk (T. Hyde), phenshall@brookes.ac.uk (P. Henshall), p.c.eames@lboro.ac.uk (P. Eames), r.moss@warwick.ac.uk (R. Moss), stan.shire@warwick.ac.uk (S. Shire), j.uhomoibhi@ulster.ac.uk (J. Uhomoibhi).

https://doi.org/10.1016/j.solener.2021.02.040
Received 1 October 2020; Received in revised form 10 February 2021; Accepted 15 February 2021
Available online 13 April 2021

work was gas leakage in the seal between the glass cover and the casing.

A vacuum flat plate solar collector proposed (Eaton and Blum, 1975), where a moderate vacuum (~150–3500 Pa) was used to minimize the convective heat loss from a solar absorber encapsulated in a vacuum enclosure, resulted in a highly efficient solar collector capable of operating at high temperatures and suitable for cold climates and weak sunlight.

A flat plate prototype collector was fabricated and tested at outdoor facilities (Benz and Beikircher, 1999). The collector exhibited high efficiencies of more than 60% at 100 °C steam temperature and 45% at 150 °C steam temperature. In another work it was demonstrated that the efficiency of a conventional collector can be increased from 25% to 60–65% for a VFP collector when operating at 150 °C above ambient temperatures (Moss and Shire, 2014).

To supply solar process heat at temperatures in the range of 120–150 °C a non-tracking, flat, low-concentrating collector was proposed (Buttinger et al., 2010). To minimise convective heat loss, a partial vacuum (<0.01 mbar) is provided using polysulphide and polybutyl rubber as sealing materials. Due to outgassing of the components, an internal pressure rise of 6 kPa is estimated after 20 years. A prototype of such a design exhibited efficiencies of about 50% at a temperature of 150 °C.

A comprehensive review has been undertaken on flat vacuum collector development over the past ten years showing a growing interest in this type of solar collector (Colangelo et al., 2016) while several patents have been filed on vacuum flat plate collectors (Estes et al., 1975; Soleau, 1981; Benvenuti, 2011; Palmieri, 2009, 2012). In these studies, particular attention has been given to the importance of the sealing methodology (sealing the cover glass to the body of the collector) as the durability of the internal vacuum is closely dependent on how strong, hermetic and vacuum compatible the seal is. A hermetic seal will prevent permeation of gas to the vacuum, and a mechanically strong seal will withstand stresses induced by atmospheric pressure and temperature differentials. In addition, a vacuum compatible sealing material will have minimal outgassing resulting in a durable vacuum (Arya, 2014).

In this work, a proprietary solder, Cerasolzer 217, has been used as a sealing material in the fabrication of vacuum flat plate enclosures. The suitability of Cerasolzer 217 for this application in terms of mechanical strength and vacuum tightness is examined and stresses across vacuum enclosures are studied.

2. Fabrication of vacuum enclosures

The fabrication of a suitable vacuum enclosure involves several key considerations due to the necessity to achieve and maintain an adequate vacuum pressure over the lifetime of the enclosure. In addition to the general conceptual collector design geometry, these include the choice of enclosure materials, development of a mechanically strong vacuum tight seal, the design of the support structure for maintaining separation of the enclosure covers and development of a suitable pump-out arrangement for collector evacuation.

2.1. Support pillar design

The vacuum enclosure in this study consists of two glass panes hermetically sealed around their periphery to a stainless steel edge spacer; the edge spacer had a thickness of 25 mm. As the vacuum is created in the cavity therein, the glass panes will tend to bow inwards and eventually fail under the influence of atmospheric pressure, therefore an array of pillars are used to support and maintain separation of the glass panes. The vacuum space between the panes accommodates a thin solar absorber plate; the design of which must take into consideration the support pillar array. The design of support pillar arrangement (pillar diameter and separation) is discussed in detail previously (Henshall et al., 2016) and summarised here:

1. The induced stress on glass surface above a support pillar in a vacuum flat plate solar collector must not exceed 4 MPa for annealed glass and 35 MPa for tempered glass. By taking this criterion into consideration in the design of the pillar specification, glass failure can be prevented over the service life of the collector.
2. Due to compressive stresses on the internal glass surface near the edge of the support pillars, conical Hertzian fractures can occur. It is shown that if the relation between pillar radius (a) and separation (λ) follows $\lambda < 155a^{3/4}$, the compressive stress will be below that which would otherwise initiate a conical fracture.
3. Compressive stress on the support pillars must be less than the compressive strength (*S*) of the pillar material. To meet this criterion the support pillar configuration (radius and separation) for a given compressive strength must satisfy ($P\lambda^2 \leq S\pi a^2$), where P is the atmospheric pressure. Support pillars fabricated from stainless steel can withstand a compressive stress of 170 MPa.
4. Support pillars must be strong enough to avoid buckling which is accomplished if the support pillar specification satisfies $\frac{\pi^2 Ea^4}{2L^2} \leq P\lambda^2$. *L* is the length of the support pillar and E is the Young's Modulus of the pillar material.
5. The vacuum enclosure must be designed to accommodate a thin solar absorber as shown in Fig. 1, Fig. 2 and Fig. 3, therefore, a series of apertures are required in the absorber to accommodate support pillars, consequently, the effective absorbing area is reduced. By limiting the number of the pillars, the fraction of the area available within the enclosure for solar absorbance will increase. In previous studies 3% of the total area of the absorber was occupied by support pillars which resulted in a 3% power loss (Henshall et al., 2016). Fig. 4 summarises these criteria presenting support pillar specifications that can enable the development of durable vacuum enclosures. As can be seen from Fig. 1, a pump-out port, inlet and outlet pipes are attached to the edge spacer through some apertures provided in the edge spacer. All pipes and ports are made of stainless steel and welded using stainless steel welding techniques. A thin solar absorber with overall thickness of 10 mm, designed and fabricated using hydroforming techniques at the University of Warwick, was incorporated in a vacuum enclosure as shown in Fig. 1 and Fig. 2. Since the internal vacuum gap in the enclosure is 25 mm, there is a distance of 7.5 mm between the absorber and each glass pane as illustrated in Fig. 3.

In this work, the vacuum enclosure covers are made from 4 mm tempered glass panes. Support pillars, 6 mm diameter and 25.4 mm long, are fabricated from stainless steel and spaced at 60 mm intervals which meets the safety criteria presented in Fig. 4 resulting in mechanically stable vacuum enclosures.

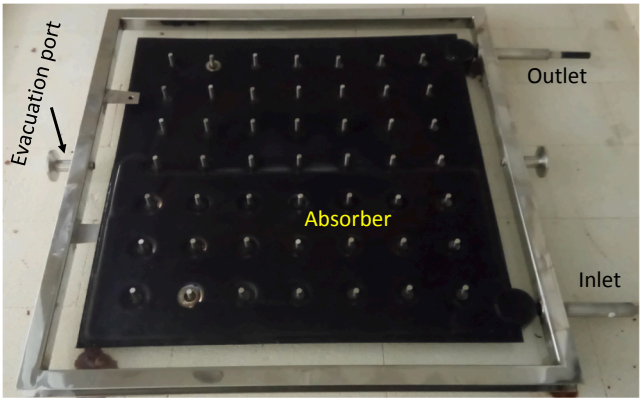

Fig. 1. Solar absorber, support pillar arrangement and edge spacer.

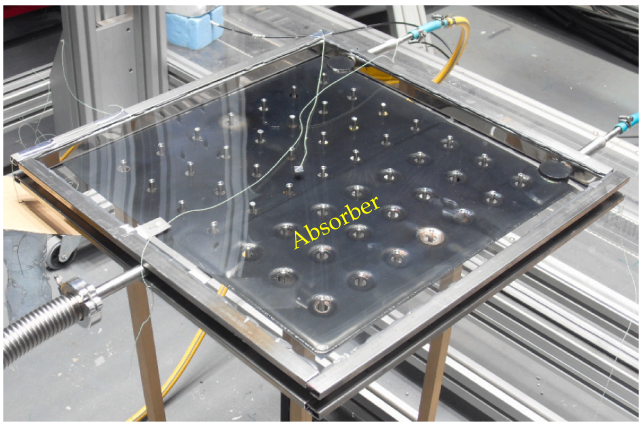

Fig. 2. Fabricated vacuum flat plate solar thermal collectors is tested under a solar simulator. A slim solar absorber was incorporated in the vacuum enclosure. The solar absorber was 10 mm thick.

2.2. Sealing techniques

The fabrication of a vacuum enclosure requires the formation of a hermetic seal between an edge spacer and glass panes and the establishment of a vacuum (less than1 Pa) between the panes. A sealing technique developed and characterised in this work is discussed in this section. Ultrasonic soldering techniques can be used to deposit thin layers of metal alloys as a sealing material on substrates such as glass. This is a flux free method of soldering where ultrasonic energy removes oxide films from the substrate surface. This method is clean and eco-friendly in comparison with conventional soldering techniques where flux is applied. High-frequency vibration breaks up oxide films and cleans the surfaces allowing the molten solder to wet and bond to the substrates. Vibrational energy forces molten solder into any micro holes creating a strong bond between the solder and the substrate (Bellex datasheet, 2016). Ultrasonic soldering techniques with indium as a sealing material have been used for the fabrication of vacuum glazing in which a high vacuum (<0.001 mbar) is created and maintained (Hyde et al., 2000; Arya et al., 2012; Fang et al., 2013). However, having a relatively low melting point (156 °C) indium may not be suitable for solar applications as the stagnation temperature for solar collectors may be higher than 156 °C (Frank et al., 2015). In addition, a high indium price and its limited availability are challenging for wide scale use. Several sealing materials have been proposed for vacuum glazing and solar applications (Koebel et al., 2011; Benvenuti, 2010; Henshall et al., 2016). Due to low melting points and wide availability, tin alloys are extensively used as soldering materials in a range of applications.

Memon and Eames (2020) have conducted a detailed experiment in attempt to seal glass panes together in the fabrication of vacuum glazing. The sealing material was a Lead-free metal alloy: Sn90-In10 (wt%). The sealing was undertaken at 450 °C and the process involved using ultrasonic soldering techniques and glass surface treatment with B2O338-Sn62 wt%. Several vacuum glazing samples were fabricated and pumped down and a minimum pressure of 8.2×10^{-4} mbar was achieved. The problem with this sealing technology is that the minimum pressure (8.2×10^{-4} mbar) is just low enough for vacuum glazing (Koebel et al., 2010; Collins et al., 1995) but considering outgassing issues this pressure may not guarantee a long lasting vacuum. One effective way of testing the level of vacuum is to evaluate the thermal transmittance (U-value) of vacuum glazing samples, however, in that work this was not experimentally done. There is no report of the mechanical strength of this seal. In addition, due to the small size of the internal space of vacuum glazing, the vacuum pressure should easily reach below 10^{-5}mbar in a short period of time (Arya, 2014), however, the minimum achievable pressure in these samples (8.2×10^{-4} mbar) indicates that there might be some leaks; no Helium mass spectroscopy was undertaken to detect leaks. Another big issue with this sealing technique is that the sealing process is happening at 450 °C; this temperature will prevent the use of tempered glass panes in the fabrication of vacuum glazing or solar collectors.

In another work, Memon et al. (2019) also used Sn-Pb-Zn-Sb-AlTiSiCu composite as a sealing material in the fabrication of vacuum glazing. In vacuum glazing samples (300 mm by 300 mm) fabricated in this work a minimum pressure of 4.2×10^{-4} mbar was achieved; this may indicate that some leaks existed, however, no Helium mass spectroscopy was undertaken to investigate the vacuum tightness of the seals. There is no report of any edge seal failure during the evacuation of vacuum glazing samples of this size (300 mm by 300 mm), however, the level of

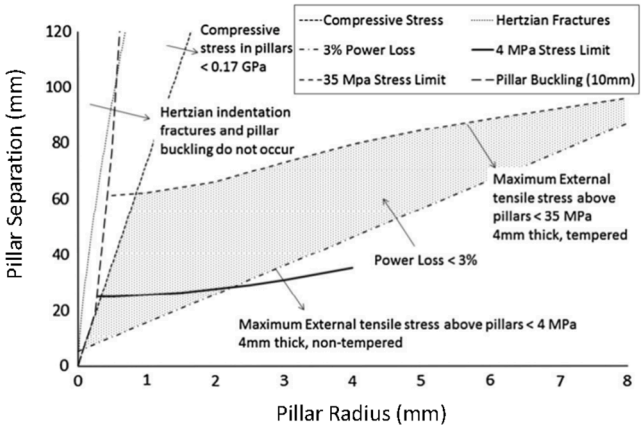

Fig. 4. Support pillar specification for 4 mm tempered and annealed glass (Henshall et al., 2016).

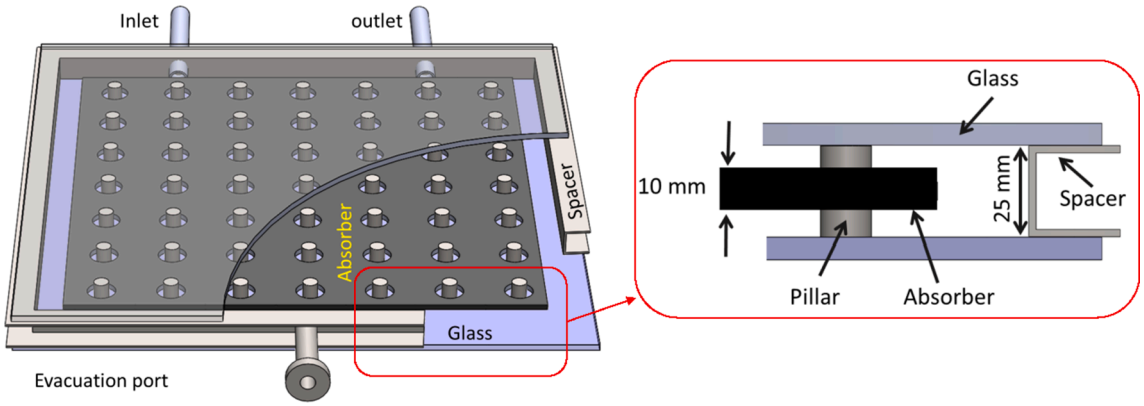

Fig. 3. Schematic diagram of vacuum enclosure with a slim solar absorber.

mechanical stress in the edge seal region will be larger in larger samples.

Mientkewitz et al. (2012) introduced an effective glass-metal sealing technique in which a metal (Ni-Cr-Si-Mn-Fe-Al) was bonded to glass where both metal and glass had similar thermal expansions. This technique was developed in particular for vacuum-tube solar collectors but it is possible to use it in other applications. The sealing process is undertaken at high temperatures as glass needs to be melted to bond to the metal to create hermetic seals. This method, therefore, cannot be used with tempered glass meaning that it may not be suitable for vacuum flat plate solar collector applications.

Yaniv et al. (1981) experimented sealing of glass to metal (cobalt–nickel-iron alloy (KOVAR)) in which a novel method of metal surface treatment was used. The seal was hermetic but the process was a high temperature process preventing the use of tempered glass. An attempt was made to lower the sealing temperature of glass to KOVAR (Wang et al., 2020); however, they managed to reduce the temperature down to 500 °C by using low melting solder glass. This sealing temperature is still too high to use tempered glass in the fabrication of solar collectors. Another issue is that the cost of KOVAR is high and may not be suitable for most applications including vacuum flat plate solar collectors.

In the fabrication of vacuum glazing, laser welding technique was used to create a hermetic seal between glass panes (Benson, 1998); however, the fabricated vacuum glazing samples did not exhibit a satisfactory U-value meaning that the vacuum pressure was not low enough. In addition, the sealing process was a high temperature process preventing the use of tempered glass.

Recently an attempt made by Zhang et al. (2020) to use laser to bond solder glass (frit) to glass pieces. This method may have some applications but not suitable for the fabrication of vacuum glazing or solar collectors as it is a high temperature process preventing the use of tempered glass. In addition, this method might bring about localized stresses in the seal.

Other attempts (Richter et al., 2015; Miyamoto et al., 2007) also made to use laser to create glass-glass seals but they are not suitable for vacuum glazing or solar collector applications as they are high temperature processes and result in localized stress.

This paper focusses on the use of a tin based alloy, Cerasolzer 217, in a sealing methodology developed for the fabrication of flat vacuum enclosures. Helium mass spectroscopy is undertaken to find out whether the seal is hermetic. Finally, different tests are performed to measure the mechanical strength of the seal. The sealing process has three stages; i) deposition of layers of Cerasolzer 217 on the collector glass covers and metal edge spacer, ii) sealing the cover glasses to the edge spacer by reflow of the deposited layers and iii) application of a secondary seal. These three steps are discussed in the following sections.

2.3. Cerasolzer deposition on substrates

Cerasolzer 217 is a vacuum compatible and lead-free metal alloy with a melting point of 217 °C. It can create a strong bond with both glass and stainless steel (Bellex datasheet, 2016). Using an ultrasonic soldering iron, a thin layer of Cerasolzer 217 is deposited around the periphery of the collector glass cover panes and the edge spacers as shown in Fig. 5. The deposited layers are approximately 0.2 mm thick and 15 mm wide. During the soldering process the glass panes and the edge spacer are heated on a temperature controlled hot plate at 150 °C and 185 °C respectively, with a soldering iron tip temperature of 300 °C. It is found that at temperatures lower than this, the molten Cerasolzer may not flow and bond to the substrates. During soldering process, circular movement of the iron tip can promote wetting of the Cerasolzer on the substrates resulting in a strong bond.

2.4. Enclosure assembly

After deposition of Cerasolzer 217 on the glass panes and edge spacer an array of support pillars are placed on the lower glass pane spaced at 60 mm intervals on a regular square Cartesian grid. The stainless steel edge spacer is positioned on the lower glass pane and the upper pane is located on the spacer so that the Cerasolzer layers are aligned as shown in Fig. 6. The assembly is heated in a bake out oven to a temperature of 250 °C, at which the seal is formed by Cerasolzer reflow.

Heating the assembly at 250 °C for 30 min creates a strong bond between the glass and the spacer; the test procedure for this is discussed in section 2.7. By limiting the sealing process temperature to 250 °C the tempered properties of the glass panes are not affected. During the soldering of Cerasolzer 217 to glass or stainless steel (or indeed most substrates), thin oxide films are formed on the surfaces of deposited layers (Bellex datasheet, 2016). During subsequent edge sealing of glass to the edge spacer, these oxide films can act as a barrier preventing the Cerasolzer layers from fusing with each other, which may affect the integrity of the seal between the layers. In addition, the oxide films inhibit molten Cerasolzer reflow, consequently, the molten layers on the

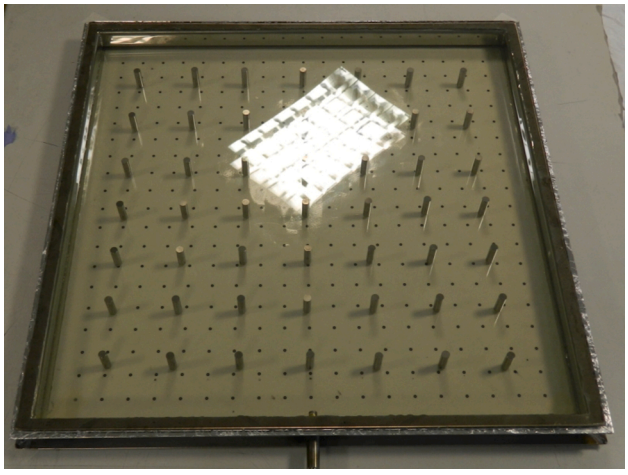

Fig. 6. Vacuum enclosure assembly before heating in a bake out oven.

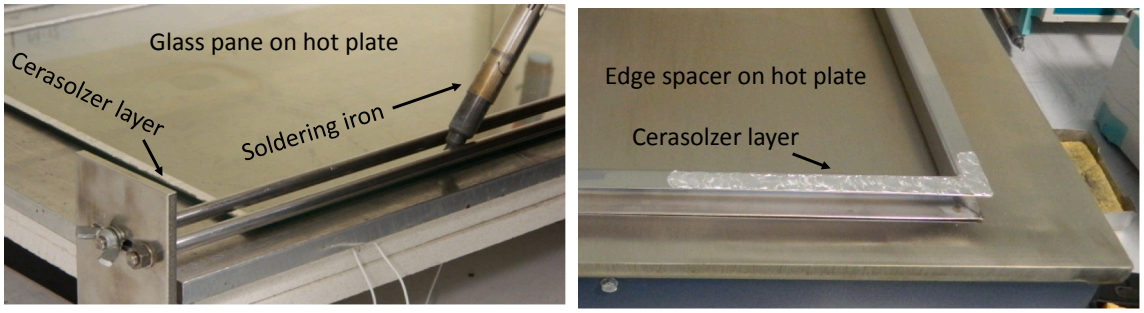

Fig. 5. Depositing Cerasolzer 217 around the periphery of collector glass cover and stainless steel spacer.

glass panes and the edge spacer may not combine to create a hermetic seal. To overcome these challenges a uniform pressure is applied in the edge seal region during the sealing process in the bake out oven to break the oxide films and promote a hermetic bond between the glass and edge spacer. This is illustrated in Fig. 7 where spring clamps are used to apply pressure to the edge seal region; however, in commercial production line laminating vacuum bags might be used instead of clamps to apply a uniform pressure as using clamps would not be practical. In this work, several vacuum enclosures were fabricated using this methodology, however, an ultimate vacuum pressure of 9.6×10^{-3} mbar was achieved indicating that the seal was not hermetic despite no visible gaps in the seal. To overcome this issue, a secondary seal is applied as discussed in the following section.

2.5. Secondary sealing

The vacuum enclosure edge seal must remain hermetic (leak-free) to ensure the stability of the internal vacuum pressure over the service life of the collector enclosure. As discussed in section 2.4, achieving a vacuum pressure lower than 9.6×10^{-3} mbar in the enclosure made with Cerasolzer 217 proved problematic. To address this issue a secondary seal was created over the seal (primary seal) as schematically shown in Fig. 8. Secondary sealant materials such as epoxy resins are commonly available, however, as these materials exhibit high outgassing rates their suitability is limited. Vacuum compatible materials such as indium, indium alloys or Cerasolzer 217 as discussed previously have been used to create hermetic seals in vacuum devices (Arya et al., 2018a). In this work Cerasolzer 217 is used for this purpose and applied with ultrasonic soldering techniques.

To apply the secondary seal, the vacuum enclosure is heated at 150 °C and held at a 45° angle to facilitate the soldering process as illustrated in Fig. 8. To investigate the hermeticity of the overall edge seal, a vacuum enclosure (shown in Fig. 9) is leak tested using a conventional Helium mass spectrometer leak detector (Ishii et al., 1983). The small scale enclosure, 0.2 m × 0.2 m, is fabricated with the application of a primary and secondary seal. The enclosure consists of two 4 mm glass panes and a stainless steel spacer (15 mm thick and 10 mm wide). An array of stainless steel support pillars (15.2 mm high and 6 mm diameter) prevent the glass panes from collapsing under the influence of atmospheric pressure. A pump-out hole of 4 mm in diameter is used for evacuation of the enclosure. As shown in Fig. 9, the leak rate varied between 10^{-1} mBar L/s and 10^{-5} mBar L/s. As the sealing process is undertaken manually, the leak rate around the periphery of the seal is non uniform. However, the leak detection analysis highlighted that areas of the edge seal do not exhibit any leaks indicating it should be possible to create a leak-free seal around the entire periphery of the vacuum enclosure using a fully automated technique.

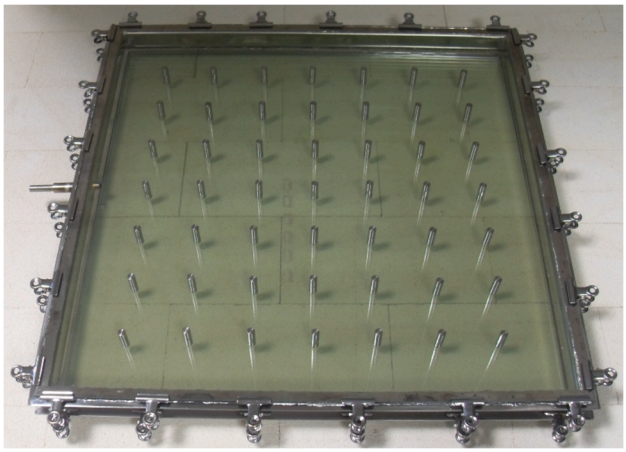

Fig. 7. Applying uniform pressure on edge seal region using clamps.

In this work, a further investigation is made to create a hermetic edge seal using ultrasonic energy during the bake out stage which is discussed in the following section.

2.6. Application of ultrasonic energy during bake out

Although the sealing process discussed in the previous section can create a hermetic enclosure, it has essentially two stages. To avoid the application of the secondary seal (second stage), an attempt is made to develop a single stage process whereby ultrasonic energy is also used to break the oxide films while a uniform pressure is applied during the bake out stage. The heating regime for cerasolzer reflow is the same as before (250 °C for 30 min) and a uniform pressure is applied in the same way as illustrated in Fig. 7. The ultrasonic energy (20 KHz) is generated by a Branson Digital Sonifier (model: 450) shown in Fig. 10.

Fig. 10 illustrates how ultrasonic energy is applied to the sealing area. Using this method, a vacuum enclosure is fabricated and subsequently evacuated. A vacuum pressure of 9.1×10^{-4} mbar was achieved indicating that the application of ultrasonic energy can improve the quality of the seal but did not result in a hermetic seal. In addition, the application of ultrasonic energy creates a vibration that can move and disperse the support pillars which is an irreversible issue (note: the pillars are not bonded to the glass panes). Further work is required to evaluate the effect of the application of ultrasonic energy during bake out stage on the mechanical strength of the bond but investigating this issue is not the focus of this paper. Due to the limitations discussed, this technique is not used in the fabrication of vacuum enclosures in this study.

2.7. Mechanical strength of edge seal

The edge seal for vacuum enclosures must be mechanically strong to withstand the stresses induced by atmospheric pressure, temperature differentials, wind loads and physical impacts. An experimental investigation is undertaken to test the strength of the Cerasolzer 217 seal between the glass panes and stainless steel spacer. Glass samples 100 mm × 50 mm (4 mm thick annealed glass) are sealed to stainless steel plates as shown in Fig. 12 creating a 50 mm × 10 mm seal area. In this section three different tests are discussed where the first test was designed to determine the best heating regime, the second and third tests were designed to investigate the strength of the seal against torque and shear stress, respectively; samples used in these tests were prepared using the sealing method described in Section 2.4.

2.7.1. Determining heating regime

To determine the best heating regime, several samples were prepared in a bake out oven under different heating regimes i.e. different temperature and different heating time. Samples are divided in ten sample groups as shown in Table 1. The samples were tested using the method described in section 2.7.2. Using each heating regime eight samples were prepared and tested; their average strength are presented in Table 1. As can be seen, samples heated at 250 °C or higher temperature for 30 min or longer time exhibit high mechanical strength; at above 130 N the glass broke. In terms of time and temperature efficiency, the best results were achieved for the samples heated at 250 °C for 30 min, consequently, in this work this heating regime is used in the fabrication of vacuum enclosures.

2.7.2. Torque test

Due to the influence of atmospheric pressure, the glass panes tend to bend towards the vacuum space as illustrated in Fig. 11. The innermost edges of the edge spacer (shown as points A and B in Fig. 11) act as fulcrums resulting in a torque force in the edge region. During evacuation of the enclosure, the torque force can initiate a failure in the seal. To evaluate this scenario a test was designed as illustrated in Fig. 12 to determine the maximum torque that can be applied to the edge seal

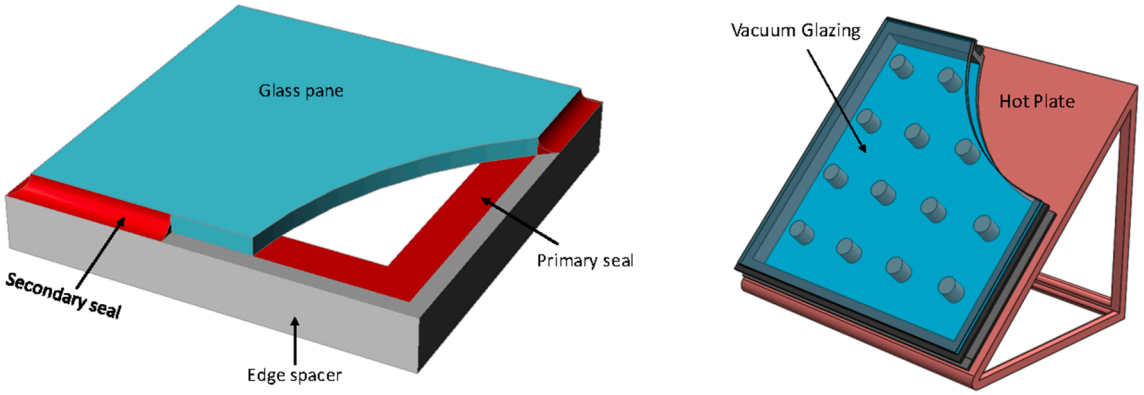

Fig. 8. Primary and secondary seal.

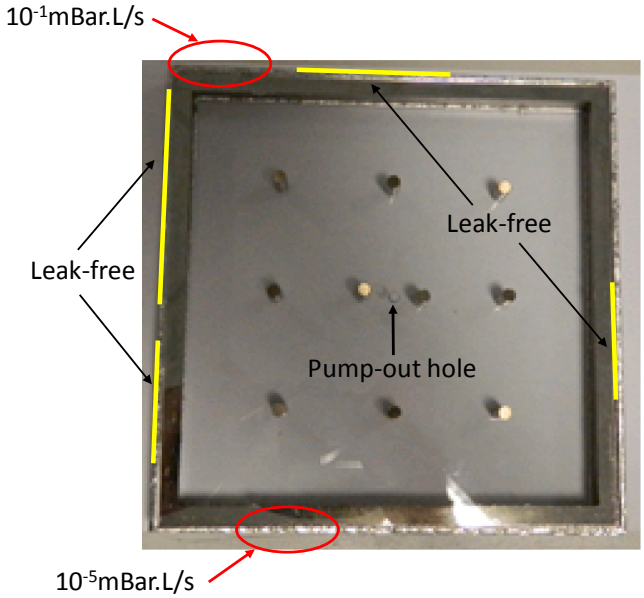

Fig. 9. Vacuum enclosure (0.2 m × 0.2 m) leak tested using a Helium mass spectrometer leak detector.

before failure occurs. As illustrated in Fig. 12, the stainless steel plate of the test sample is fixed along the lower surface while a load is applied to the free end of the glass plate.

To ensure the repeatability of the test results, eight samples were prepared at 250 °C for 30 min and tested against applied torque; the results for these tests are presented in Table 2. During testing, failure occurred each time in the glass plate, however, the seal did not fail. The variability in failure load is due to the unique defect profile of each glass sample.

The tests showed that the smallest failure load for the glass is 122 N corresponding to a torque given by:

$$\tau = F \times L = 10.98 \text{ N m}$$

where $F = m \times g = 148$ N and L is the effort arm which is 90 mm as illustrated in Fig. 11.

The torque at the edge region is calculated to investigate whether the torque created by atmospheric pressure at the edge seal region of a vacuum enclosure is large enough to result in failure of the seal or glass. In the vacuum enclosures fabricated in this work, the distance between the edge spacer and the first raw of pillars is 90 mm, hence the effective effort arm is 45 mm. The total torque applied on every W length of the edge seal in the enclosures is given by:

$$\tau = F \times L = (A \times P) \times L \Rightarrow d\tau = (dA \times P) \times (x), dA = W \times dx \Rightarrow \tau$$
$$= \int_0^L W \times dx \times P \times x = 5.13 \text{ N m}$$

where P is atmospheric pressure (101325 N/m^2) and x is the distance from the fulcrum as shown in Fig. 12. As the test samples are 50 mm wide, for comparison purpose W is also considered to be 50 mm. The torque applied on every 50 mm of edge seal (5.13 N m) is less than the lowest torque value (10.98 N m) that resulted in failure of the glass indicating that atmospheric pressure will not induce a failure in either the glass or the edge seal for the vacuum enclosure configuration used in this work. As the edge seal in the fabricated vacuum enclosures is wider (15 mm) than the seal in the test samples (10 mm) it may be concluded

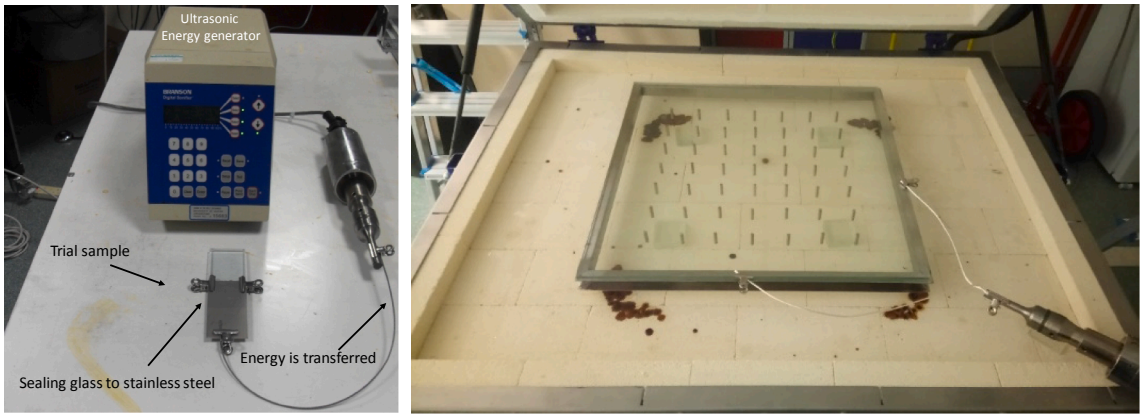

Fig. 10. Ultrasonic energy is applied to the sealing region.

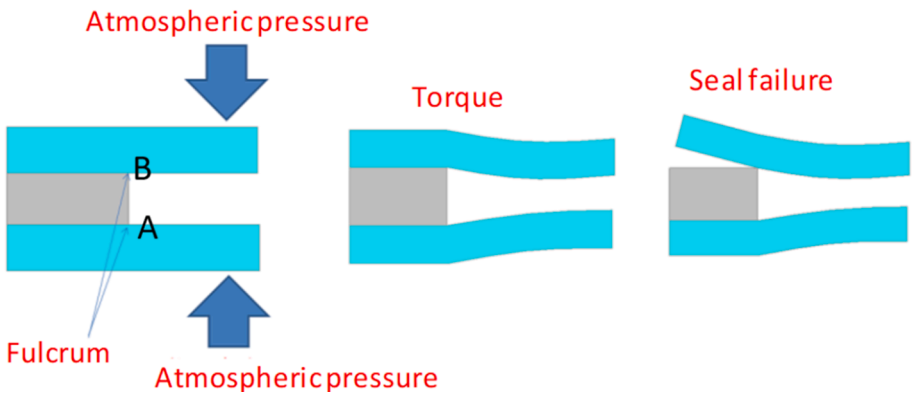

Fig. 11. Torque due to atmospheric pressure.

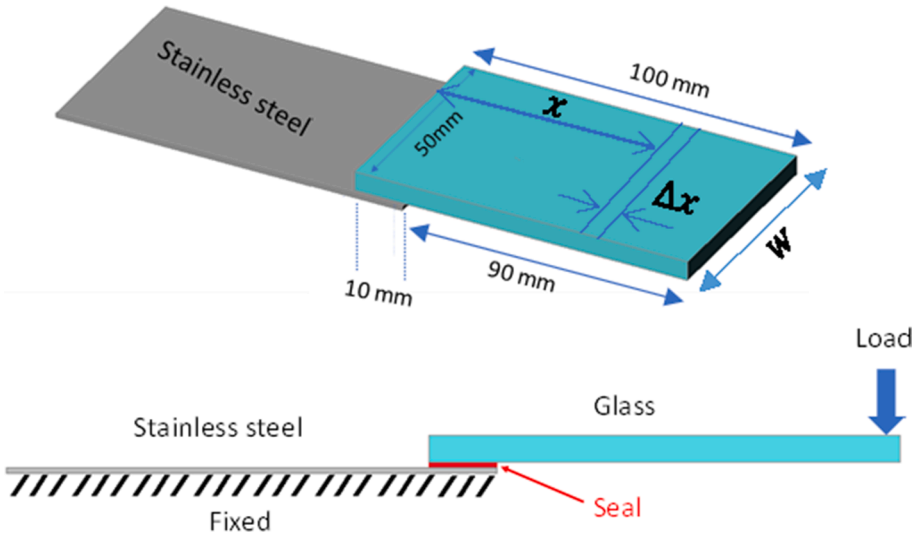

Fig. 12. Schematic diagram of testing a sample for torque resistance.

that the seal in the vacuum enclosure can withstand the stresses induced by the atmospheric pressure load.

Although Cerasolzer 217 has been shown to provide a strong bond between the glass and edge spacer, an additional support bracket is added to the enclosures as illustrated in Fig. 13. These brackets provide further mechanical support against the stresses in the edge seal region, and protect the glass edges from mechanical impact as tempered glass panes are vulnerable at their edges. The brackets are made of 1.5 mm thick stainless steel and attached to the enclosure using an epoxy resin.

2.7.3. *Shear test*

To ensure repeatability of the sealing process using the adopted heating regime (250 °C for 30 min), eight samples were tested against shear stress using a tensometer shown in Fig. 14b. Due to tensile force, the glass in all samples failed while the seal remained intact (Fig. 15) indicating that the mechanical strength of the seal against shearing force is higher than that of glass.

2.8. *Pump-out of vacuum enclosure*

To suppress gaseous convective and conductive heat transfer a vacuum pressure less than 1 Pa must be created between the panes. A turbo molecular vacuum pump is connected to the enclosure via a vacuum port welded through the edge spacer as shown in Fig. 13a. During the evacuation process, the enclosure is heated to 150 °C for 7 h in a bake-out oven to outgas the internal surfaces enabling a higher ultimate vacuum pressure to be achieved and help prolong the service life of the enclosure. The selection of heating temperature and duration of evacuation is based on previous studies on vacuum glazing (Arya et al., 2014); however, further research is required to determine the relation between these two factors for vacuum enclosures. When bake-out and evacuation are completed, the pump-out port is sealed using a novel technique discussed in detail in the following sections.

The pump-out port comprises a standard KF-25 flange attached to a stainless steel tube with an inner diameter of 10 mm as illustrated in Fig. 16; however sealing a tube with this diameter is challenging. The technique developed in this work is suitable for sealing pump-out ports with inner diameters of around 1 mm however, pump-out ports with such a small diameter may adversely affect the effectiveness of evacuation process.

The impact of the internal tube diameter on the effectiveness of the evacuation process was investigated for pump-out ports with internal diameters including 10 mm, 8 mm, 4 mm, 2 mm and 1 mm. The test set-up and the evacuation rates are presented in Figs. 17 and 18, respectively. To ensure repeatable test conditions for each port, a vacuum gauge is installed to a 10 mm port on one edge of the enclosure and an evacuation port is selected on the opposite edge, for example, Port B2 is connected to the vacuum gauge and port C is connected to the vacuum pump.

A turbo molecular vacuum pump (T-Station 75 EDWARDS with pumping rate of 42 L/s) is used for evacuation; the results presented in Fig. 18 are valid for this arrangement. It should be noted this is a

Table 1
Mechanical strength of the bond between glass and stainless steel created by Cerasolzer 217 using different heating temperature and heating time.

Sample	Temperature (°C)	15′	30′	45′	60′	Time (m)
Sample Group 1	217	17	18	18	20	**Applied Forces (N)**
Sample Group 2	220	15	17	18	17	
Sample Group 3	230	67	94	107	101	
Sample Group 4	240	89	121	117	127	
Sample Group 5	250	92	137	134	137	
Sample Group 6	260	94	136	136	133	
Sample Group 7	270	95	132	134	133	
Sample Group 8	280	94	137	136	135	
Sample Group 9	290	96	135	134	137	
Sample Group 10	300	95	132	135	131	

(Arya et al., 2014, 2018a,b; Beikircher et al., 2015; Benz et al., 1996; Benz and Beikircher, 1999; Buttinger et al., 2010; Colangelo et al., 2016; Collins et al., 1995; Eaton and Blum, 1975; Fang et al., 2013; Fang and Arya, 2019; Henshall et al., 2016; Hyde et al., 2000; Koebel et al., 2010, 2011; Memon et al., 2019; Memon and Eames, 2020; Miyamoto et al., 2007; Moss et al., 2017, 2018a–e; Richter et al., 2015; Schneider et al., 2012; Yaniv et al., 1981; Zhang et al., 2020; Abbott and Madocks, 2001; Arya et al., 2012; Arya et al., 2018c; Arya, 2014; Bellex datasheet, 2016; Benvenuti, 2010; Benvenuti, 2011; BS EN 12150; DANTEC-Dynamics, 2014; Estes et al., 1975; Frank et al., 2015; Ishii et al., 1983; Mientkewitz et al., 2012; Moss and Shire, 2014; Palmieri, 2012; Palmieri, 2009; Soleau, 1981; Wang et al., 2020).

comparative analysis; if a vacuum pump with a different pumping speed is used, the absolute values will be different. The vacuum gauge used in this work is Leybold: PTR 90 PENNINGVAC.

The test results show that the size of the inner diameter of the pump-out port is directly proportional to the evacuation rate. Using the pump-out ports with inner diameters of 1 mm and 10 mm, the required pressure for solar applications (less than 0.01 mbar) is achieved within 150 min and 15 min, respectively for a 0.5 m × 0.5 m × 0.0254 m enclosure. Evacuating the enclosure through a 1 mm port does not provide an optimized time efficient solution, however, as the pump-out speed is not a critical aspect of this study a pump-out port with an inner diameter of 1 mm was used to ease port sealing. The pump-out port sealing technique required a novel port design having a variable diameter of 10 mm reducing to 1 mm as shown in Fig. 19 where the evacuation rate is determined by the smaller diameter. A piece of a sealing material (e.g. Cerasolzer 217 or indium) is placed in the larger section of the port as illustrated in Fig. 19. The sealing material does not does not conform to the shape of the evacuation port and evacuation is possible. When the required vacuum pressure has been achieved the pump-out port is sealed by local induction heating of the seal material which accumulates at the bottom of the larger port section blocking the narrow outlet. Sealing is achieved as the molten material cannot penetrate the small diameter hole, resulting in a vacuum tight seal. To ensure the seal is vacuum tight, the pump-out port is exposed to ultrasonic energy during heating in a similar manner to that described in section 2.6. To protect the metal seal from moisture, a secondary seal can be applied. Further research is required to test the long term durability of the vacuum in the enclosure.

3. Study of vacuum enclosure structure

3.1. Vacuum enclosure components

The design and components of vacuum enclosures must be able to withstand the stresses caused by atmospheric pressure loads, temperature differentials and other mechanical impacts. The support pillar arrangement (spacing and diameter) and materials must be able to counteract the pressure imposed on the glass covers by atmospheric pressure. Support pillars manufactured from stainless steel, with a diameter of 6 mm and a spacing of 60 mm were used in this project to fulfil this criterion, as discussed in Section 2.1.

The edge seal fulfils a crucial role in the integrity of vacuum enclosures. In addition to providing hermeticity, it must be mechanically strong to withstand stresses in the edge seal region. In the previous work, it was shown that an edge seal formed by Cerasolzer 217 using an ultrasonic soldering technique was able to withstand stresses caused by both atmospheric pressure and temperature differentials of 20 °C. The vacuum enclosure exhibited no leaks or catastrophic failure when exposed to solar insolation levels of 780 W/m^2 for 7 h (Arya et al., 2018a; 2018b). In this work, further investigations are undertaken on the mechanical strength of the edge seal (reported in Section 3.3).

Finally, the glass covers must be able to withstand the induced stresses. If the glass surface is flat and the pillars have a uniform height,

Table 2
Failure load for test samples.

	Sample 1	Sample 2	Sample 3	Sample 4	Sample 5	Sample 6	Sample 7	Sample 8	**Average**
Load (N)	130	135	145	146	148	123	122	148	**137.125**

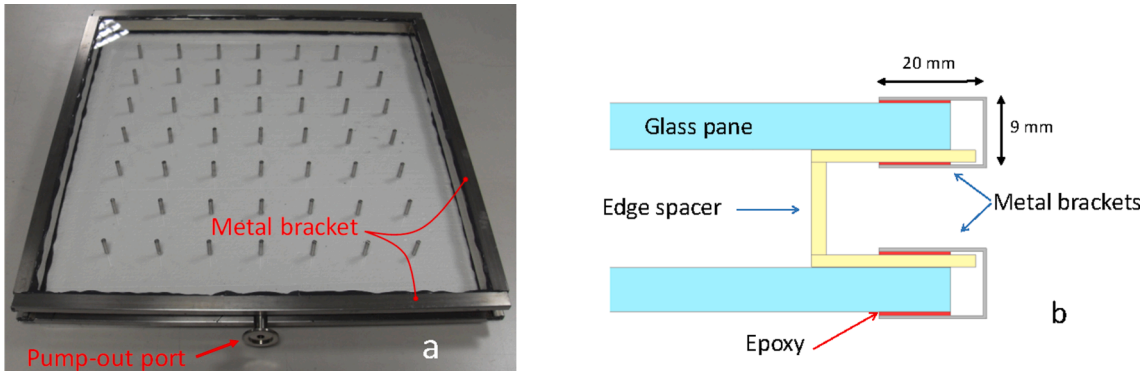

Fig. 13. Completed vacuum enclosure (a), U-shape section added to enclosure (b).

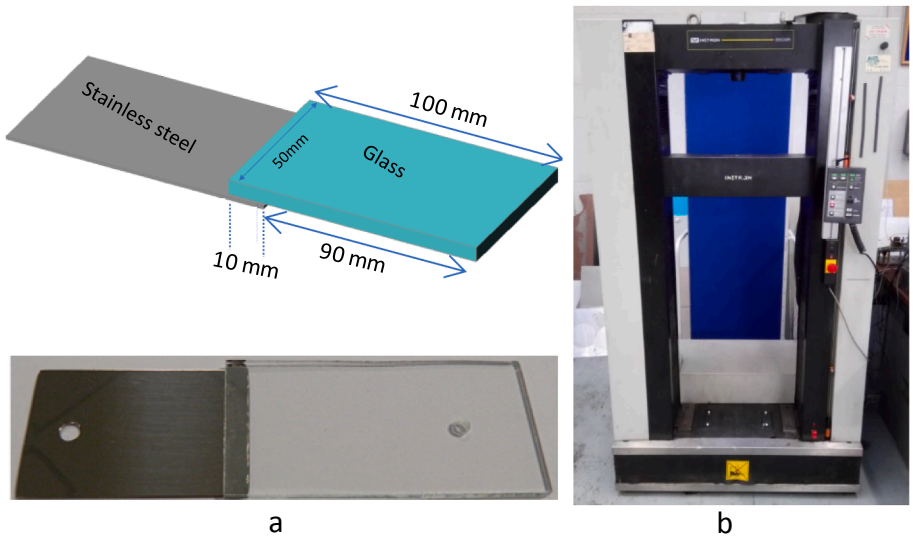

Fig. 14. Test samples (a) tensometer (b).

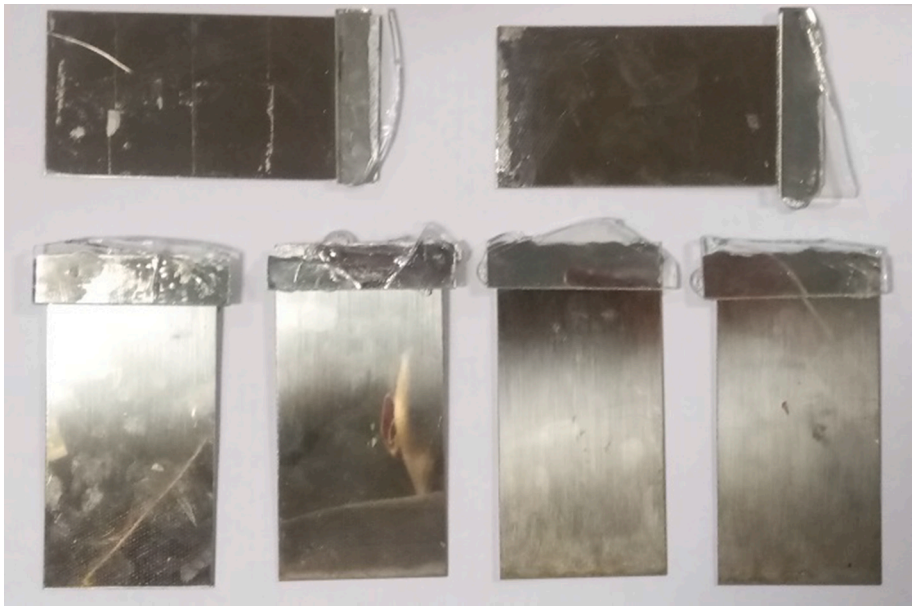

Fig. 15. Samples after testing for shear strength of edge seal.

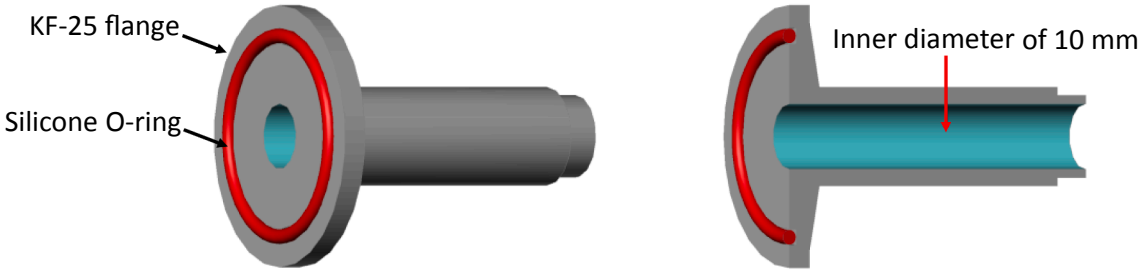

Fig. 16. Schematic diagram of pump-out port.

the force from atmospheric pressure will be uniformly distributed over the pillars (Henshall et al., 2016); however, if there are variations in pillar height, longer pillars will experience higher loads resulting in increased stress in the glass in these regions and a potential for failure of the glass covers. Fig. 20 shows a vacuum enclosure fabricated from 4 mm thick annealed glass. Annealed float glass panes have flat surfaces but due to differences in support pillar height (±0.2 mm resulting from manufacturing error), the atmospheric load was unequally distributed between the pillars resulting in high stress concentrations in specific locations in the glass covers which lead to glass failure as shown in

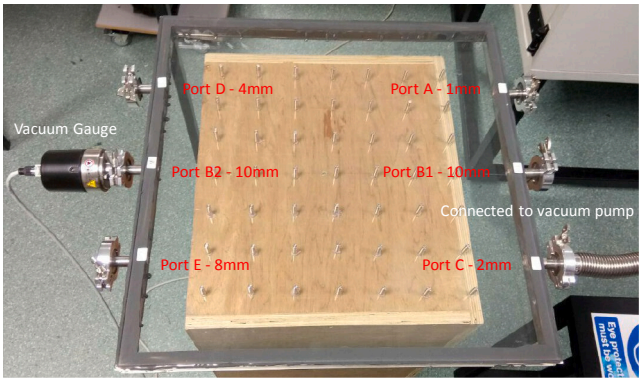

Fig. 17. Test set-up designed to investigate evacuation rate (Internal dimension: 0.5 m × 0.5 m × 0.025 m).

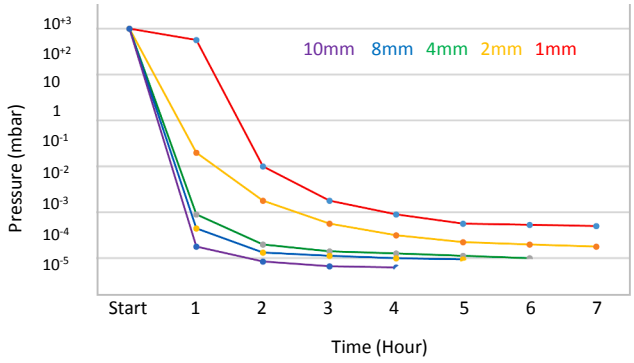

Fig. 18. Evacuation rates for pump-out tubes with different inner diameters.

Fig. 20.

In this work, tempered glass panes have been used in the fabrication of vacuum enclosures. Thermally tempered glass panes offer additional mechanical strength; however, they are not flat and exhibit a characteristic roller wave due to the tempering process (Abbott and Madocks, 2001; Fang and Arya, 2019). As a result of this, the atmospheric pressure load is not uniformly distributed over the support pillars even if the pillars have the same height. To investigate the variation in stress distribution between the pillars in a vacuum enclosure made with tempered glass panes, digital image correlation (DIC) is used for preliminary experimental measurements of enclosure strain. In this test, only the stress induced by atmospheric pressure is considered.

3.2. DIC study of strain profile in vacuum enclosures

A range of vacuum enclosures were initially fabricated in this study using 4 mm annealed glass panes; however, during evacuation 80% of enclosures suffered glass pane failure. Consequently, fabrication of vacuum enclosures concentrated on the use of tempered glass panes. As discussed previously tempered glass does not have planar surfaces due to the tempering process, having a deviation in the range of 0.5 mm in the overall flatness for 4 mm thick glass (BS EN 12150). To analyse the impact of this, digital Image Correlation (DIC) is used to study the strain profile over the surface of a fabricated vacuum enclosure (0.55 m × 0.55 m) made with two 4 mm tempered glass panes. A Dantec Dynamics Q-400 DIC system, (shown in Fig. 21) consisting of two high resolution cameras is used to take images of the vacuum enclosure (upper glass pane) before and after the evacuation of the enclosure to a pressure 0.001 Pa. The DIC system compares those images and determines the change in strain profile of the glass resulting from a change in the loading conditions. Prior to the DIC measurement, the upper glass pane is spray coated to create a random black speckle pattern on a white background. The DIC system is calibrated using a method described by the manufacturer (DANTEC-Dynamics, 2014).

All images are taken at the same temperature (room temperature), therefore the DIC readings of strain are only associated with the effect of atmospheric pressure acting on the enclosure. The principal strain contours produced by the DIC measurement, presented in Fig. 22, follow the support pillar array pattern. As the image is taken by only one of the DIC cameras it is somewhat oblique.

In Fig. 22, the black circles present the expected locations of the support pillars underneath the upper glass pane, however, pillar centers are not exactly aligned with the centers of the peak stress detected by DIC system. This may be due to small misalignments in the actual pillar positions. Fig. 22 shows that stresses in the vicinity of the support pillars varies from pillar to pillar, for example, the stress near pillar 1 is smaller than that near pillar 2. As outlined previously this variation may be due to a non-uniformity in pillar length or due to variations in the planarity of the tempered glass pane. However, the stress variation did not result in either catastrophic failure of the enclosure or Hertzian fractures in any of the 4 mm tempered glass panes.

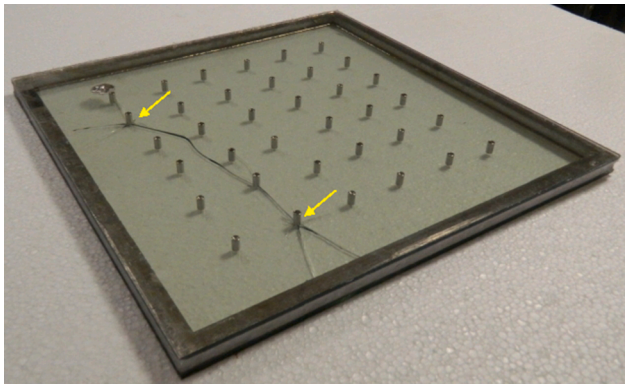

Fig. 20. Longer support pillars resulting in glass breakage in a vacuum enclosure fabricated from annealed glass.

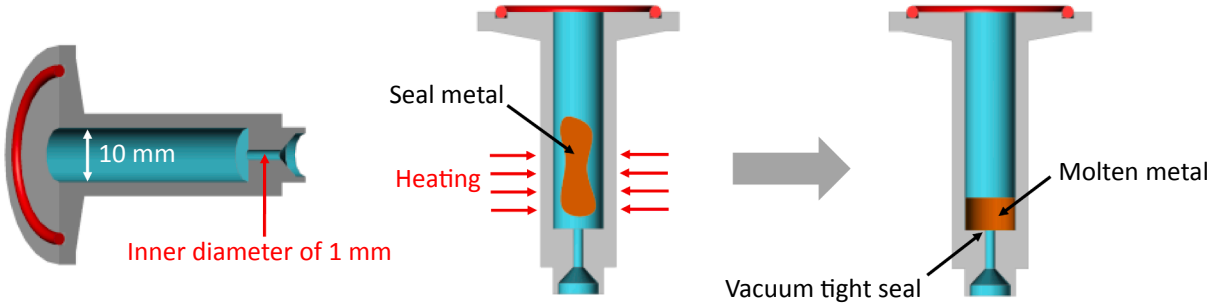

Fig. 19. Schematic diagram of sealing pump-out port.

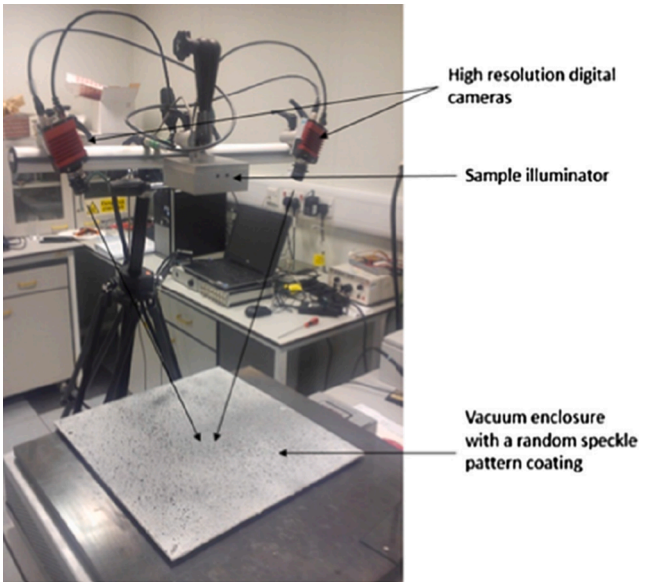

Fig. 21. DIC system setup and painted vacuum enclosure (Henshall et al., 2016).

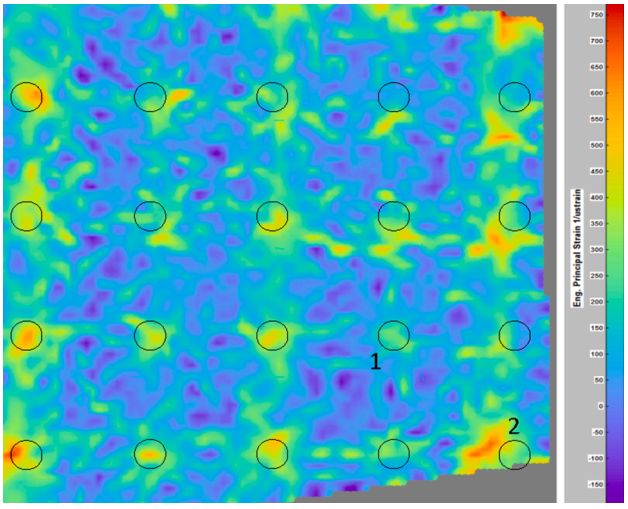

Fig. 22. DIC principal strain contours; circles represent the locations of support pillars.

3.3. Mechanical strength of enclosure

The vacuum enclosures in this study are designed for solar applications, hence they will be exposed to varying mechanical impacts from the surrounding environment. The edge seal and glass panes of the enclosures must be capable of withstanding those impacts. To investigate the resistance to a range of loads the mechanical strength of a vacuum enclosure is theoretically and experimentally analysed against a concentrated force. The effect of temperature differentials will be investigated in future work.

3.3.1. Experimental approach

Using a tensometer (Model: Instron 5500R Universal Test Frame shown in Fig. 23), a concentrated force is applied to the centre of a vacuum enclosure as illustrated in Fig. 23. The specifications for the vacuum enclosure are those as described in Section 2.1. The enclosure is located on a platform as shown in Fig. 23 which supports the enclosure around the periphery of the edge spacer only, consequently, the two glass panes are free to deflect. During this test, the machine applies a force up to 2000 N on a circular disc with a diameter of 15 mm in the centre of the enclosure. The applied force and the relevant deformation of the vacuum enclosure is presented in Fig. 24. During this test the enclosure is continuously evacuated to achieve an internal vacuum pressure of 6.7×10^{-5} mbar.

A load of approximately 2000 N was applied to the enclosure resulting in a total deflection of 5.5 mm in the center of the enclosure area. Due to atmospheric pressure acting on the glass panes and the support pillars, both panes follow the same deflection profile under loading. During the test, no edge seal failure, glass breakage or pressure rise in the internal vacuum was observed therefore the overall stress in the edge seal region caused by both atmospheric pressure and the applied force is lower than the mechanical tolerance limits of the seal. However, due to the applied force by the tensometer, additional stress is induced on the enclosure which will be theoretically investigated in the following section.

3.3.2. Theoretical approach

In this section, a 3D finite element method (FEM) software (ABAQUS) is used to evaluate the shear stress in the edge seal region and the principal stress on the external surface of glass pane directly above a support pillar. In the modelling approach, a force of 2000 N is applied to the centre region of a vacuum enclosure with the same specifications of the fabricated enclosure used in the experimental analysis. The glass panes are, realistically, assumed to be fixed to the support pillars and to the edge spacer i.e. no relative movement is assumed. The contact surface of the support pillars with the glass panes is assumed to be flat which may not be the case in practice due to machining tolerances. If support pillars have rough or uneven contact surfaces, higher stress levels will exist within the glass panes, consequently, the results from the modelling may not be representative of the experimental investigation. In the modelling process, the meshes were refined until the results from the modelling were in close agreement with the results from the experimental study (with a deviation of less than 5%).

The deflection of the enclosure was the only parameter measured during the experimental study, hence this is the only parameter used to validate the modelling; however, in future work the strain across the vacuum enclosure will be measured using micro strain gauges. For comparison purposes, the vacuum enclosure is modelled with and without the application of the concentrated force. Fig. 25a presents the deflection profile of the vacuum enclosure due to atmospheric pressure (with no concentrated force). The maximum glass deflection between support pillars away from the edge spacer is 0.5 mm. The glass deflection between the first row of pillars and the edge spacer is 1.8 mm, this is a result of the larger separation between the edge spacer and the first raw of pillars (90 mm) compared to the separation between subsequent rows of pillars (60 mm). Fig. 25b presents the deflection profile of the vacuum enclosure due to atmospheric pressure and the application of concentrated force of 2000 N. As illustrated the maximum deflection of the enclosure is 5.8 mm which is in close agreement with the experimental test result with a deviation of 5.5%. Due to atmospheric pressure the glass panes and the support pillars are in perfect contact and as a result, both glass panes have the same deflection curvature.

Bending of glass panes between support pillars as a result of atmospheric pressure causes the vacuum enclosure to shrink, consequently, the edge spacer deflects as illustrated in Fig. 26, having a maximum deflection of 0.3 mm; however, the application of the applied force (2000 N) on the centre of the enclosure reduces the deflection from 0.3 mm to 0.23 mm. This is more likely because the deflection of the enclosure counteracts the deflection of the spacer. The edge spacer is fabricated from 1.5 mm thick stainless steel sheet, however, there can be cost and weight advantages in using a lighter spacer. To investigate this, the modelling is repeated for a vacuum enclosure having an edge spacer fabricated from 0.5 mm stainless steel sheet. The modelling showed that the deflection of the edge spacer with and without the applied force (2000 N) would be 0.39 mm and 0.81 mm, respectively. It is also

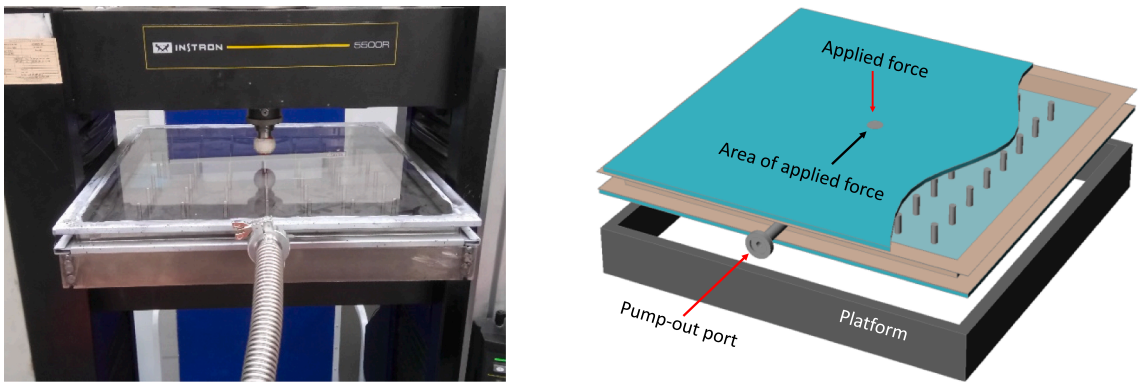

Fig. 23. Mechanical strength test set-up.

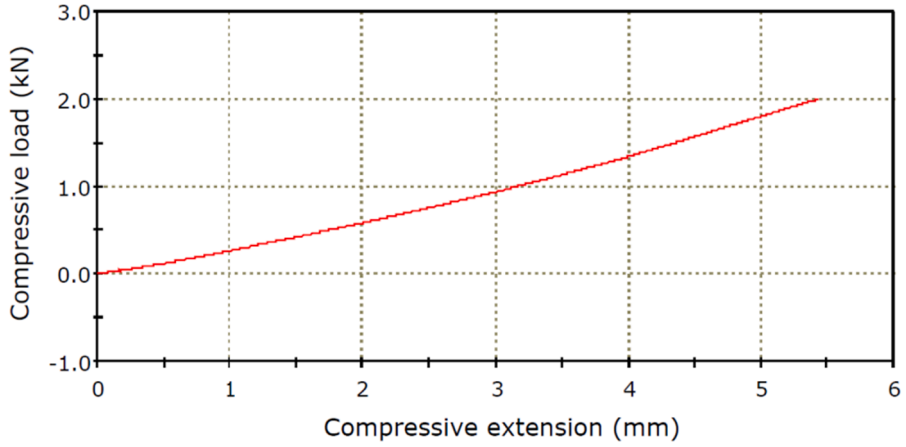

Fig. 24. Mechanical strength test results.

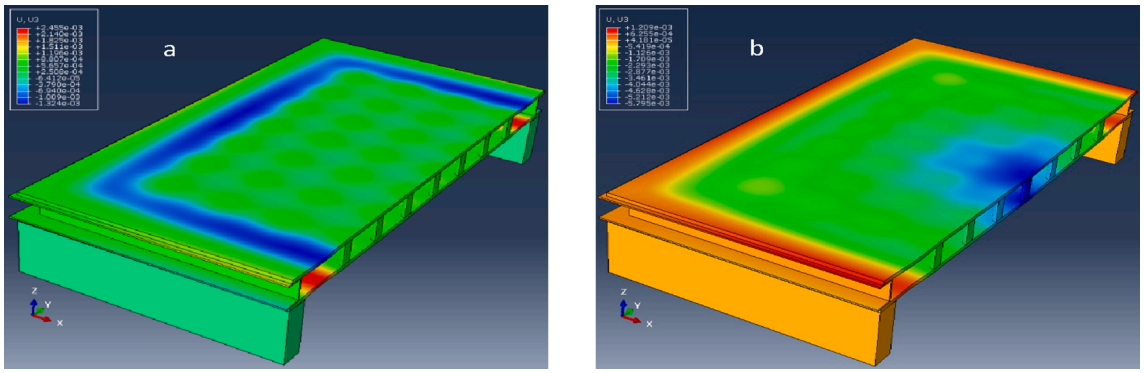

Fig. 25. Deflection profile of vacuum enclosure (a) due to atmospheric pressure (b) due to atmospheric pressure and the application of a concentrated force of 2000 N.

interesting to note that the maximum deflection of the enclosure under 2000 N is 6.3 mm for the thinner edge spacer profile. The results for the bending of the edge spacer profile and the deflection of the vacuum enclosure are similar for both profile thicknesses therefore a saving in weight and cost should be potentially possible without compromising the structural integrity of the vacuum enclosure.

Due to atmospheric pressure, the glass panes are deflected to a convex shape over the support pillars and to a concave shape between the pillars. Stress over support pillars away from the edge spacer is uniform at each pillar however the stress over the pillar in the centre of the enclosure is analysed using the FEM software as the applied load of 2000 N acts directly above this pillar. The simulation showed that the principal stress in the glass over this pillar is 21 MPa as a result of atmospheric pressure and with the applied load on the enclosure, the principal stress in the same point increases to 28 MPa. The principal stress on the glass surface over the same pillar on the lower side of the enclosure (convex side) increases to 67 MPa. No glass failure was observed in the vacuum enclosure made from 4 mm tempered glass

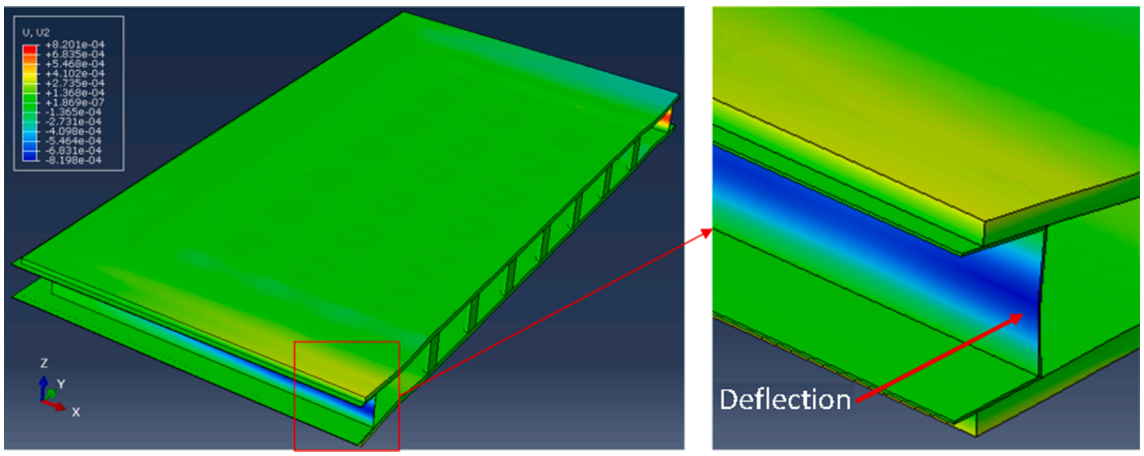

Fig. 26. Deflection of the edge spacer.

panes during the experimental study. By increasing the thickness of the glass panes the existing stresses can be reduced (Arya et al., 2018c). Fully tempered glass panes can withstand a continuous stress of 70 MPa over 30 years if a support pillar specification of 6 mm diameter and 60 mm spacing is used (Henshall et al., 2016). However, tempered glass panes are more sensitive to the formation of scratches, hence during handling and cleaning of vacuum enclosures scratching of the glass panes must be avoided to minimise the risk of glass failure (Schneider et al., 2012).

The edge seal region in vacuum enclosures experiences large and constant shear stresses which can result in edge seal failure if the stress exceeds the strength limits of the seal. The shear stress in the edge seal region is not experimentally determined in this study however it is theoretically calculated using the FEM software. The simulation showed that the shear stress varies across the edge seal region with an average stress of 0.4 MPa and a maximum of 36 MPa in the corner region close to the innermost edge of the spacer. With the applied load of 2000 N the enclosure experiences additional stresses and as a result the average shear stress increases to 0.55 MPa and the maximum shear stress increases to 43 MPa at the same locations.

The shear stress in the edge seal region of a vacuum enclosure with an edge spacer made with 0.5 mm thick stainless steel sheet is also simulated. It was found that the shear stress varies across the edge region with an average of 0.2 MPa and a maximum of 23 MPa in the corner region close to the innermost edge of the spacer and with the applied load of 2000 N the edge seal region experiences an average shear stress of 0.54 MPa, and a maximum shear stress of 31 MPa in the same regions. This indicates that the use of a lighter edge spacer for vacuum enclosures reduces shear stresses in critical regions and has the potential to improve the durability of the edge seal and life expectancy of the vacuum enclosure.

4. Conclusion

Vacuum flat plate solar thermal collectors exhibit excellent optical and thermal characteristics due to a combination of their wide surface area and high vacuum thermal insulation offering a high performance and architecturally versatile solar thermal collector which has a variety of applications for industrial process heat and for building integration.

A range of vacuum enclosures were fabricated, using a tin-based alloy, Cerasolzer 217, as a sealing material. A novel two stage sealing technique was employed to create a seal between the glass panes and edge spacer at or below 250 °C allowing the use of tempered glass without loss of temper qualities. It was demonstrated that the bond between the glass and spacer was capable of withstanding existing stresses in the edge seal region and using a conventional helium mass spectrometer leak detector, it was shown that a hermetic seal was achievable.

In this work, vacuum enclosures were fabricated from 4 mm tempered glass panes and stainless steel support pillars (6 mm diameter and 25.4 mm long) were spaced at 60 mm intervals which met the safety criteria preventing glass failure. A novel technique was developed for sealing a pump-out port with an inner diameter of 1 mm. Helium mass spectrometer leak detection showed the seal was hermetic. An experimental study was designed to investigate the impact on pumping rates from using pump-out ports with diameters between 1 mm and 10 mm. The test showed that the size of the inner diameter of the pump-out ports is proportional to the evacuation rates. Using pump-out ports with inner diameters of 1 mm and 10 mm, the required pressure for solar applications (less than 0.01 mbar) was achieved within 150 min and 15 min, respectively.

Experimental DIC measurements showed that in vacuum enclosures made with tempered glass panes the stress above support pillars varies from pillar to pillar. This variation may be due to non-uniformity in pillar length and the non-planarity of the tempered glass panes. However, the stress variation did not result in either catastrophic failure of the enclosure or Hertzian fracture failure in the glass for vacuum enclosures fabricated using 4 mm tempered glass panes.

An applied load of 2000 N in the centre of a vacuum enclosure resulted in a deflection of 5.5 mm. During the test, no edge seal failure, glass breakage or pressure rise in the internal vacuum occurred. Using a 3D finite element method (FEM) software (ABAQUS), stresses in a vacuum enclosure were calculated. The modelling was validated by the experimental results, with a deviation of 5.5%.

In vacuum enclosures, bending of glass panes between the support pillars induces deflection in the web section of the edge spacer having a maximum value of 0.3 mm when fabricated with 1.5 mm thick stainless steel, however, modelling of a vacuum enclosure with an edge spacer fabricated from 0.5 mm stainless steel showed a web deflection of 0.81 mm in the edge spacer. The application of an applied load of 2000 N to the centre of the enclosure would result in a maximum bending of 6.3 mm for the overall enclosure. These values indicate that there is no advantage in using thicker profiles in the fabrication of the edge spacer.

Simulations showed that the principal stress over the centre pillar was 21 MPa and with the application of a 2000 N load on the enclosure, the principal stress in this region increased to 28 MPa, while the principal stress on the glass surface above the same pillar on the lower side of the enclosure (convex side) increased to 67 MPa. These stresses are less than the mechanical strength of fully tempered glass panes which can withstand a continuous stress of 70 MPa over 30 years. During the test

no glass failure was observed.

It found that the shear stress in edge seal region varies across and along the edge with an average of 0.4 MPa and a maximum of 36 MPa near the corners close to the innermost edges of the spacer. By applying a force (2000 N) to the centre of the enclosure the average shear stress increased to 0.55 MPa and the maximum shear stress increased to 43 MPa (in the same region). The impact of transport has not been studied in this work, however, if the vacuum solar collector developed in this work is commercialised, a protocol for transporting and handling the system should be developed in order to avoid any damages to the system.

The shear stress in the edge seal region of a vacuum enclosure with an edge spacer fabricated from 0.5 mm stainless steel varies across the edge region with an average of 0.2 MPa, and a maximum of 23 MPa near the corner close to the innermost edges of the spacer. By applying a 2000 N force, the edge seal region experienced an average shear stress of 0.54 MPa, and a maximum shear stress of 31 MPa near the corners close to the innermost edges of the spacer. Using a thinner (0.5 mm) edge spacer profile the shear stress in the edge seal region is reduced which may improve the durability of the edge seal. In addition, the weight and cost of the enclosure is reduced.

Using Cerasolzer 217 as a sealing material and the sealing technique developed in this work, several vacuum enclosures were successfully fabricated. The methodology is reliable and reproducible and can be used in flat vacuum solar collector technology.

Declaration of Competing Interest

The authors declare that they have no known competing financial interests or personal relationships that could have appeared to influence the work reported in this paper.

Acknowledgements

The authors are grateful to the Engineering and Physical Sciences Research Council (EPSRC) for funding this work as part of a collaborative programme between the University of Warwick, Loughborough University and Ulster University, reference EP/K009915/1, EP/K010107/1 and EP/K009230/1. The authors also wish to express their graduates to Dr John Kelly and Dr Mohammad Dadashzadeh of Ulster University for their great help with setting up the experiments and completing this work.

References

Abbott, M., Madocks, J., 2001. Roller wave distortion–definition, causes and a novel approach to accurate, on-line measurement the main text. Glass Process 2001; Days Proc., 18–21.

Arya, F., Fang, Y., Hyde, T. (2012). Fabrication and characterization of Triple vacuum glazing at low temperatures using an indium – based seal. In: Proceeding of the Energy and Material Research Conference EMR; 2012. p. 521–524.

Arya, F., Hyde, T., Henshall, P., Eames, P., Moss, R., Shire, S., 2014. Fabrication and Characterisation of Slim Flat Vacuum Panels Suitable for Solar Applications. Proceedings of EuroSun 505–511.

Arya, F., Hyde, T., Henshall, P., Eames, P., Moss, R., Shire, S., 2018a. Vacuum enclosures for solar thermal panels Part 1: Fabrication and hot-box testing. Sol. Energy 174, 1212–1223.

Arya, F., Hyde, T., Henshall, P., Eames, P., Moss, R., Shire, S., 2018b. Vacuum enclosures for solar thermal panels Part 2: Transient testing with an uncooled absorber plate. Sol. Energy 174, 1224–1236.

Arya, F., Hyde, T., Trevisi, A., Basso, P., 2018. The effect of glass thickness on stresses of vacuum glazing. In: Proceeding of ICHREET 2018c (International Conference on Home Renewable Energy and Efficiency Technologies), London, UK, Oct 15 – 16.

Arya, F., 2014. Developing alternative sealing materials in fabrication of evacuated glazing at low temperature. PhD Thesis. Ulster University; 2014. http://ethos.bl.uk/OrderDetails.do?uin=uk.bl.ethos.629079.

Beikircher, T., Möckl, M., Osgyan, P., Streib, G., 2015. Advanced solar flat plate collectors with full area absorber, front side film and rear side vacuum super insulation. Sol. Energy Mater. Sol. Cells 141, 398–406.

Bellex datasheet. http://www.bellexinternational.com/products/cerasolzer/; 2016 [accessed 28 Oct 2016].

Benvenuti, C., 2010. Evacuable flat panel solar collector. US Patent 2010; US 7810491 B2.

Benvenuti, C., 2011. Evacuated solar panel with a non evaporable getter pump. US Patent 2011; US20110155125A1.

Benz, N., Beikircher, T., 1999. High efficiency evacuated flat-plate solar collector for process steam production. Sol. Energy 65, 111–118.

Benz, N., Beikircher, T.H., Aghazadeh, B., 1996. Aerogel and krypton insulated evacuated flat-plate collector for process heat production. Sol. Energy 58, 45–48.

BS EN 12150: Glass in building – Thermally toughened soda lime silicate safety glass.

Buttinger, F., Beikircher, T., Pröll, M., Schölkopf, W., 2010. Development of a new flat stationary evacuated CPC-collector for process heat applications. Sol. Energy 84, 1166–1174.

Colangelo, G., Favale, E., Miglietta, P., de Risi, A., 2016. Innovation in flat solar thermal collectors: a review of the last ten years experimental results. Renew. Sustain. Energy Rev. 57, 1141–1159.

Collins, R.E., Turner, G.M., Fischer-Cripps, A.C., Tang, J.Z., Simko, T.M., Dey, C.J., Clugston, D.A., Zhang, Q.C., Garrison, J.D., 1995. Vacuum glazing – a new component for insulating windows. Build. Environ. 30 (4), 459–492.

DANTEC-Dynamics, 2014. Q-400 Systems Operation Manual.

Eaton, C.B., Blum, H.A., 1975. The use of moderate vacuum environments as a means of increasing the collection efficiencies and operating temperatures of flat-plate solar collectors. Sol. Energy 17, 151–158. https://doi.org/10.1016/0038-092X(75)90053-5.

Estes, J.M., Kerlin, E.E., Blum, H.A., 1975. Flat plate solar collector module. US Patent 1975; US3916871A.

Fang, Y., Arya, F., 2019. Evacuated glazing with tempered glass. Sol. Energy 183, 240–247. https://doi.org/10.1016/j.solener.2019.03.021.

Fang, Y., Hyde, T., Arya, F., Hewitt, N., 2013. A novel building component hybrid vacuum glazing-a modelling and experimental validation. ASHRAE 119, Part 2.

Frank, E., Mauthner, F., Fischer, S. (2015). Overheating prevention and stagnation handling in solar process heat applications. 2015; IEA SHC Task 49, Technical Report A.1.2.

Henshall, P., Eames, P., Arya, F., Hyde, T., Moss, R., Shire, S., 2016. Constant temperature induced stresses in evacuated enclosures for high performance flat plate solar thermal collectors. Sol. Energy 127, 250–261.

Hyde, T.J., Griffiths, P.W., Eames, P.C., Norton, B., 2000. Development of a novel low temperature edge seal for evacuated glazing. In: Proceeding of World Renewable Energy Congress VI. Pergamon, pp. 271–274.

Ishii, H., Seki, K., Morishita, H., Yamazaki, T., 1983. Leakage detection method using Helium. US Patent 1983; US4419882A.

Koebel, M.M., Hawi, N.E., Lu, J., Gattiker, F., Neuenschwander, J., 2011. Anodic bonding of activated tin solder alloys in the liquid state: a novel large-area hermetic glass sealing method. Sol. Energy Mater. Sol. Cells 95, 3001–3008.

Koebel, M.M., Manz, H., Emanuel Mayerhofer, K., Keller, B., 2010. Service-life limitations in vacuum glazing: a transient pressure balance model. Sol. Energy Mater. Sol. Cells 94 (6), 1015–1024.

Memon, S., Eames, P.C., 2020. Design and development of lead-free glass-metallic vacuum materials for the construction and thermal performance of smart fusion edge-sealed vacuum glazing. Energy Build. 227, 110430.

Memon, S., Fang, Y., Eames, P.C., 2019. The influence of low-temperature surface induction on evacuation, pump-out hole sealing and thermal performance of composite edge-sealed vacuum insulated glazing. Renew. Energy 135, 450–464. https://doi.org/10.1016/j.renene.2018.12.025.

Mientkewitz, G., Schaffrath, W., Köhler, T., 2012. Glass-metal connection, in particular for a vacuum-tube solar collector, United States patent US 8,097,318, 2012 Jan 17.

Miyamoto, I., Horn, A., Gottmann, J., Wortmann, D., Yoshino, F., 2007. Fusion welding of glass using femtosecond laser pulses with high-repetition rates. J. Laser Micro/Nanoeng. 2, 57–63.

Moss, R., Shire, S., Eames, P., Henshall, P., Hyde, T., Arya, F., 2018a. Design and commissioning of a virtual image solar simulator for testing thermal collectors. Sol. Energy 159, 234–242.

Moss, R., Shire, S., Henshall, P., Arya, F., Eames, P., Hyde, T., 2018b. Performance of evacuated flat plate solar thermal collectors. Thermal Sci. Eng. Progr. 8, 296–306.

Moss, R.W., Henshall, P., Arya, F., Shire, G.S.F., Eames, P.C., Hyde, T., 2018c. Simulator testing of evacuated flat plate solar collectors for industrial heat and building integration. Sol. Energy 164, 109–118.

Moss, R.W., Henshall, P., Arya, F., Shire, G.S.F., Hyde, T., Eames, P.C., 2018d. Performance and operational effectiveness of evacuated flat plate solar collectors compared with conventional thermal, PVT and PV panels. Appl. Energy 216, 588–601.

Moss, R.W., Shire, G.S.F., Henshall, P., Eames, P.C., Arya, F., Hyde, T., 2018e. Design and fabrication of a hydroformed absorber for an evacuated flat plate solar collector. Appl. Therm. Eng. 138, 456–464.

Moss, R.W., Shire, G.S.F., Henshall, P., Eames, P.C., Arya, F., Hyde, T., 2017. Optimal passage size for solar collector microchannel and tube-on-plate absorbers. Sol. Energy 153, 718–731.

Moss, R.W., Shire, G.S.F., 2014. Design and performance of evacuated solar collector microchannel plates. In: Conference Proceedings of EuroSun, 2014, Aix-les-Bains (France), 16–19 September 2014, http://proceedings.ises.org/paper/eurosun2014/eurosun2014-0039-Moss.pdf.

Palmieri, V., 2012. Method of producing vacuum solar thermal panels with a vacuum tight glass-metal seal. US Patent 2012; US8161645B2.

Palmieri, V., 2009. Vacuum solar thermal panel with radiative screen. Australian Patent 2009; AU2009295584A2.

Richter, S., Zimmermann, F., Eberhardt, R., Tünnermann, A., Nolte, S., 2015. Toward laser welding of glasses without optical contacting. Appl. Phys. A – Mater. 121, 1–9.

Schneider, J., Schula, S., Weinhold, W.P., 2012. Characterisation of the scratch resistance of annealed and tempered architectural glass. Thin Solid Films 520, 4190–4198. https://doi.org/10.1016/j. tsf.2011.04.104.

Soleau, B.S. Thin-line collectors. US Patent 1981; US4282862A.

Wang, Z., Gao, Z., Chu, J., Qiu, D., Niu, J., 2020. Low Temperature Sealing Process and Properties of KOVAR Alloy to DM305 Electronic Glass. Metals 2020, 10, 941; doi: 10.3390/met10070941.

Yaniv, A.E., Katz, D., Klein, I.E., Sharon, J., 1981. New technique of surface preparation for bonding glass to KOVAR. Glass Technol. 22 (5), 231–235.

Zhang, S., Kong, M., Miao, H., Memon, S., Zhang, Y., Liu, S., 2020. Transient temperature and stress fields on bonding small glass pieces to solder glass by laser welding: numerical modelling and experimental validation. Sol. Energy 209, 350–362. https://doi.org/10.1016/j. solener.2020.09.014.